Journal of Power Sources 196 (2011) 1886–1893

Contents lists available at ScienceDirect

Journal of Power Sources

journal homepage: www.elsevier.com/locate/jpowsour

Modification of Ni-based cathode material for molten carbonate fuel cells using Co_3O_4

Young-Suk Kim[a], Cheol-Woo Yi[b,*], Hee Seon Choi[a], Keon Kim[a,**]

[a] Department of Chemistry, Korea University, Seoul 136-701, Republic of Korea
[b] Department of Chemistry and Institute of Basic Science, Sungshin Women's University, Seoul 136-742, Republic of Korea

ARTICLE INFO

Article history:
Received 15 May 2010
Received in revised form 13 July 2010
Accepted 14 August 2010
Available online 14 October 2010

Keywords:
Molten carbonate fuel cell
Cathode material
Solubility
Lithiation
Neutron diffraction

ABSTRACT

The degradation of cathode materials due to the so-called 'NiO dissolution' problem, is one of the most critical issues restricting the long-term operation of molten carbonate fuel cells (MCFCs). To overcome this problem, a modified NiO powder is prepared by the annealing of a pre-mixed powder consisting of Ni powder and Co_3O_4 nano-particles (n-Co_3O_4) at 650 °C. Annealing above 300 °C plays an important role in converting the physically bound mixed oxide system to a chemically bound system and, therefore, the separation of n-Co_3O_4 from Ni is prevented. This modification leads to the formation of a $Ni_{0.9}Co_{0.1}O$ solid solution, and the lithiated $Ni_{0.9}Co_{0.1}O$ has a core–shell structure that consists of different Li contents. Whereas the core phase has a low concentration of lithium, the outer layer is a highly lithiated phase. Since the highly lithiated outer phase, acting as a barrier, minimizes the dissolution of NiO, the modified cathode demonstrates good electrochemical properties and chemical stability under actual operating conditions. This study can provide an effective way to mass produce MCFC cathode materials.

1. Introduction

Molten carbonate fuel cells (MCFCs) are currently under development for use as power sources and are expected to function as efficient energy-conversion devices in the near future [1,2]. Typically, an MCFC uses a molten alkali carbonate mixture as the electrolyte and is operated at 650 °C, a temperature at which the molten carbonate mixture has sufficient ionic conductivity. Due to its high operating temperature, the MCFC has many advantages. For instance, the fast kinetics at high temperature makes it possible to provide sufficient electrochemical activity without any additional noble metal catalyst, and even fuels containing impurities such as CO and/or hydrocarbons can be directly used in MCFC operation without further purification. Moreover, the MCFC is suitable for coal gas utilization, because of its efficient use of waste heat, and as a result, it has been widely applied to large-scale stationary power generation and other applications.

Although the NiO electrode is the cathode material that is presently employed in MCFCs, it has a critical problem with its long-term stability. Degradation of the cathode materials due to the so-called 'NiO dissolution' problem limits the long-term operation of MCFCs [2]. Initially, NiO is slowly dissolved in the mixture of molten carbonates and the dissolved Ni ions diffuse toward the anode through the electrolyte, where they encounter hydrogen and are reduced to metallic nickel. Simultaneously, the reduction of the Ni concentration in the electrolyte induces the continuous dissolution of NiO. The degradation of the cathode leads to an increase in overpotential and the accumulative deposition of metallic Ni on the matrix, consequently causing a short-circuit due to the contact between the two electrodes. Various materials [3–11], such as $LiFeO_2$, $LiCoO_2$, $LiCoO_2$–$LiFeO_2$–NiO and some mixed oxides, have been widely studied to overcome the degradation problem of the cathode. Even though these materials demonstrate better stability in a molten carbonate mixture in comparison with NiO, they still have some drawbacks, such as poor electrical conductivity and high cost. Hence, modification of the NiO electrode has been studied extensively to overcome these limitations [1,12–26].

Surface modification of the electrode material to render it more stable is considered to be the most effective method for improving the surface properties and maintaining the bulk properties. Various coating materials have been reported [1,12–18,20–26], but cobalt is the most commonly used coating material because it forms a more stable phase, $LiCoO_2$, in the electrolyte than NiO and $Li_xNi_{1-x}O$ [18,20,22–24,26]. Even though, in the authors' previous studies [1,22,23], Co-coated NiO cathodes showed good stability and maintained good performances, additional complex coating processes are essential to prepare Co-coated NiO electrodes and organic

* Corresponding author. Tel.: +82 2 920 7666; fax: +82 2 920 2047.
** Corresponding author. Tel.: +82 2 953 1172; fax: +82 2 953 1172.
E-mail addresses: cheolwoo@sungshin.ac.kr (C.-W. Yi), kkim@korea.ac.kr (K. Kim).

0378-7753/$ – see front matter © 2010 Elsevier B.V. All rights reserved.
doi:10.1016/j.jpowsour.2010.08.086

materials are employed in the coating process which restricts their large-scale fabrication.

In the present study, the cathode material is modified without resorting to any complex coating process. The NiO powders modified with Co_3O_4 were investigated using various analytical techniques. It is obvious that this modified NiO forms a $Ni_{0.9}Co_{0.1}O$ solid solution and that the lithiated $Ni_{0.9}Co_{0.1}O$ has a core–shell structure with two different phases having different concentrations of lithium. The physical and electrochemical properties of the modified cathode material were thoroughly investigated, and finally it is discussed how this modified NiO enhances its stability in the molten carbonate electrolyte.

2. Experimental

2.1. Preparation of cathode materials

The cathode materials were prepared using Co_3O_4 particles. Specifically, to examine the effect of the particle size of Co_3O_4, Co_3O_4 powders with different sizes were pre-mixed with Ni powder (particle size = 2.2–2.8 μm, Inco nickel 255) by ball-milling, and then the mixture was directly added to the slurry [23]. The mole ratio of Co to Ni was fixed at 10 mol% throughout the study. The slurry consists of a solvent (ethanol:toluene = 70:30 wt.%, Junsei), a binder (polyvinyl butyral, Monsanto), a plasticizer (dibutyl phthalate, Junsei), a dispersant, and a defoamer. A green sheet was fabricated by tape-casting and dried at room temperature for 24 h. Then, it was sintered at 750 °C in a reducing atmosphere for 30 min. The resulting cathodes modified with *n*-Co_3O_4 (particle size ~30 nm, Aldrich) and *m*-Co_3O_4 (particle size ~1–2 μm, Aldrich) are referred to as the *n*-cathode and *m*-cathode, respectively. Both the cathodes show partial agglomeration of cobalt. In order to minimize this agglomeration, the Ni powder and *n*-Co_3O_4 were pre-mixed by ball-milling and the powder thus obtained was annealed at various temperatures from 200 to 650 °C for 10 h before mixing with the slurry. The cathodes were prepared in the same manner as that described above. For the control experiments, Co-coated and pristine NiO cathodes are used as reference cathodes. The Co-coated cathode was prepared by the Pechini method using the same procedure as that described in elsewhere [23].

2.2. Characterization of cathode materials

The morphology of the powder samples and prepared cathodes was observed by field emission-scanning electron microscopy (FE-SEM, Hitachi S-4300), and the distribution of cobalt was determined by energy dispersive spectroscopy (EDS, Horiba EX-200) coupled with SEM. In order to elucidate the structure of the material, the prepared samples were investigated by powder X-ray diffraction (XRD) using a Rigaku DMAX-III diffractometer equipped with a Cu target and neutron diffraction with a high resolution powder diffractometer (at HANARO in KAERI, Ge-monochromator, λ = 1.83523 Å). The behavior of the prepared materials under actual MCFC operating conditions was investigated by the lithiation test and by solubility measurements. The experimental devices and procedures are shown elsewhere in detail [20,23,26]. The prepared cathode is oxidized at 650 °C for 10 h and 1.5 g of the cathode material and 100 g of $(Li_{0.62}K_{0.38})_2CO_3$ are used. Initially, CO_2 was blown at 500 °C for 24 h and then a CO_2/O_2 (0.67/0.33 atm) gaseous mixture was blown at 650 °C. Subsequently, the cathode material was immersed in the molten carbonate mixture. For the lithiation test, after a desired period of time, the cathode material was withdrawn from the molten carbonate. The residual carbonates on the surface of each sample were removed using 1.0 M acetic acid, and then the powder was rinsed with distilled water and dried in an oven. For a solubility measurement, ~0.3 g samples were periodically collected. The solidified carbonates were completely dissolved in hydrochloric acid. The concentration of Ni dissolved in the carbonate was measured by inductively coupled plasma-mass spectroscopy (ICP-MS, Elan DRC II, Perkin Elmer).

2.3. Electrochemical measurements

The performance of cells with the various cathodes was examined by a unit-cell test performed at 650 °C. The unit cell consisted of a porous Ni–10 wt.% Cr plaque (Twin Energy, Korea), Li/K carbonates (62/38 mol%; Twin Energy, Korea) and porous γ-$LiAlO_2$ (Twin Energy, Korea) that served as the anode, electrolyte and matrix, respectively. A H_2/CO_2 (0.8/0.2 atm) gaseous mixture humidified by steam at 50 °C and CO_2/O_2 (0.67/0.33 atm) were provided to the anode and cathode, respectively. The total pressure of each gaseous mixture was fixed at 1 atm. Electrochemical impedance spectroscopy (EIS) was used to investigate the electrochemical properties of the prepared cathode materials. The test cell was assembled with two nominally identical electrodes, and this configuration minimized the influence of the counter electrode and obviated the need for a reference electrode [12,27]. The pellet-type electrode was prepared by cold-pressing, followed by oxidation at 650 °C for 10 h. A gold wire was attached to the pellet using silver paste and these materials were protected by ceramic adhesive to avoid the direct contact of the Au lead and silver paste with the electrolyte. The EIS test was carried out in $(Li_{0.62}K_{0.38})_2CO_3$ at 650 °C under CO_2/O_2 (0.67/0.33 atm) gaseous conditions with an IM6 electrochemical instrument (ZAHNER Elektrik, Germany).

3. Results and discussion

3.1. Particle-size effect of Co_3O_4 powder

First, to find the optimum size of the Co_3O_4 powder, Co_3O_4 powders with different sizes were pre-mixed with Ni powder and then the mixture was directly added to the slurry. As a reference, a 10 mol% Co-coated NiO cathode (referred to as the Co-coated cathode) was prepared by the Pechini method [23]. The morphology and cobalt distribution of the prepared cathode materials are shown in Fig. 1. The Co-coated cathode prepared by the Pechini method has a morphology that is similar to the pristine NiO cathode and shows a homogeneous distribution of cobalt. Even though the morphology of the *n*-cathode has a similar to that of the coated one, partial agglomeration of cobalt is observed, as shown in Fig. 1. In addition, the solubility tests were performed for 300 h, and the results demonstrate that the *n*-cathode exhibits enhanced stability (15.08 ppm of Ni) in the mixture of molten carbonates in comparison with the NiO cathode (30.35 ppm). Even if Ni dissolution of the *n*-cathode is greatly reduced, its value is slightly higher than that of the Co-coated cathode (12.71 ppm) [23], probably due to the agglomeration of Co on the surface of the cathode material. On the other hand, the *m*-cathode shows the worst distribution of cobalt among the various electrodes.

The performance of the unit cells with the prepared cathodes is shown in Fig. 2. The average open-circuit voltages (OCVs) of the unit cells with the different types of cathode are almost the same, viz., ~1.1 V. The closed-circuit voltages (CCVs, at 150 mA cm^{-2}), however, vary in the range of 0.80–1.00 V. After ~150 h, the Co-coated cathode shows the highest performance (1.00 V) among the various cathodes, which is superior to that of a commercial NiO cathode (0.95 V). Even though the performance of the *n*-cathode is slightly lower (0.98 V) than the coated cathode, it is still higher than that of a commercial NiO electrode. The performance of the *m*-cathode, however, is much lower than that of the others. This low

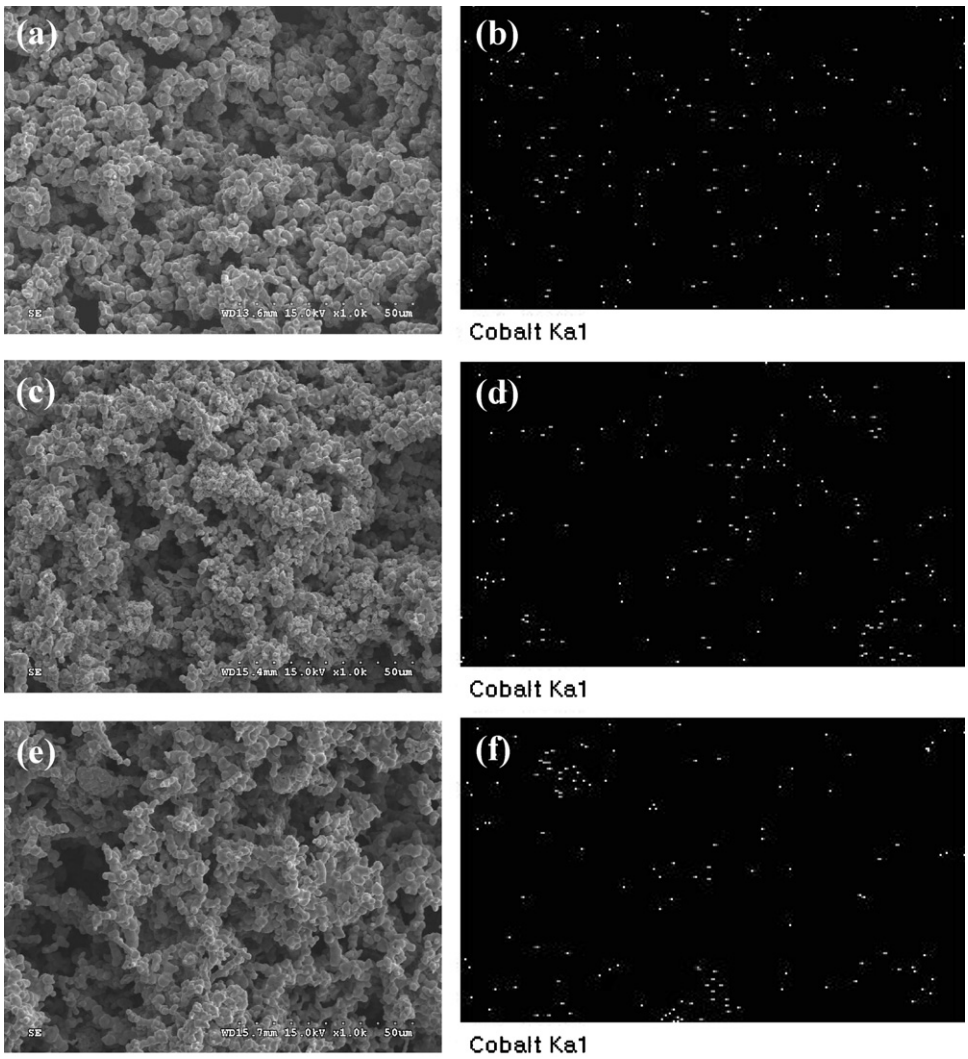

Fig. 1. SEM and cobalt mapping images of (a) coated cathode, (b) cobalt mapping image of (a), (c) *n*-cathode, (d) cobalt mapping image of (c), (e) *m*-cathode, and (f) cobalt mapping image of (e). Scale bar represents 50 μm.

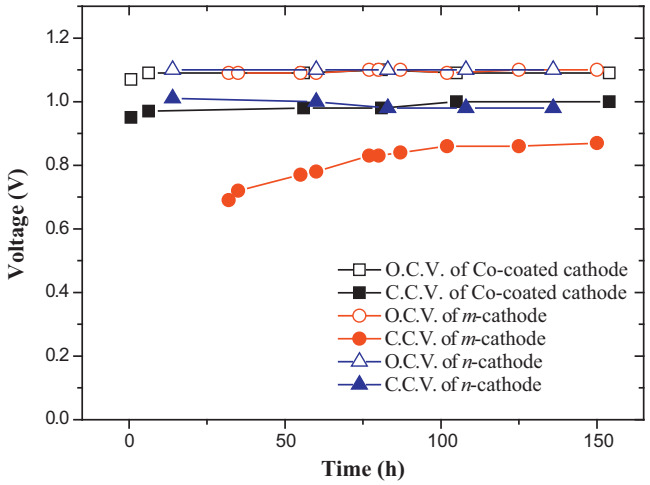

Fig. 2. Unit-cell performance of various cathodes. CCV is measured at a current density of 150 mA cm^{-2}.

performance is attributed to the agglomeration of cobalt, because it reduces the effect exerted by the addition of cobalt, in comparison with that which would be exerted by the actual amount of cobalt, and the agglomerated Co particles are the less-conducting parts of the electrode. Practically, even if *m*-Co_3O_4 powder is easily made by mechanical grinding, it is difficult to prepare a sample in which the Co particles effectively cover the surface of the Ni particles, since their sizes are similar to, or larger than, that of the Ni powder. In contrast to the *m*-Co_3O_4 powder, the *n*-Co_3O_4 powder completely covers the Ni powder, and the *n*-cathode demonstrates good stability and performance, which are comparable with those of the Co-coated cathode.

3.2. Modified cathode material

In the previous section, it was shown that the performance of the *n*-cathode is slightly lower than that of the Co-coated cathode, probably due to the agglomeration of cobalt. The agglomeration of cobalt may originate from detachment of the Co_3O_4 nano-particles from the Ni particles during the mixing process. In order to confirm this, the *n*-Co_3O_4 on the Ni particles was further investigated. The SEM and EDS images of the Ni powder pre-mixed with *n*-Co_3O_4 (10 mol% of Co) after ball-milling for 24 h are shown in Fig. 3. It is found that *n*-Co_3O_4 completely covers the Ni particles and that the

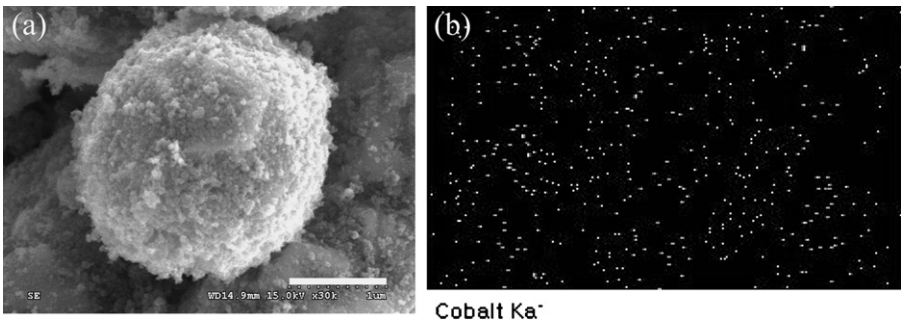

Fig. 3. SEM and mapping images of Ni powder mixed with n-Co_3O_4 (10 mol%); (a) SEM image and (b) cobalt mapping of (a). Scale bar represents 1 μm.

distribution of cobalt is homogeneous without any complex coating process being used. At this stage, however, the Co_3O_4 particles are just physically deposited on the surface of the Ni particles.

To investigate the behavior of the pre-mixed powder in the slurry, dispersion tests were conducted. The stoichiometrically pre-mixed powder prior to or after oxidation at 200 – 650 °C was immersed in 5.0 mL of a solvent, which had the same composition as the slurry (ethanol:toluene = 70:30 wt.%), and then ultra-sonicated for 1 min. Whereas the pristine and Co-coated NiO powder is not dispersed at all and sunks quickly in the solvent, n-Co_3O_4 does not sink and remains dispersed in the solvent even after 24 h. In the case of the pre-mixed powder without oxidation and oxidized below 300 °C, the deposited n-Co_3O_4 is separated from the Ni particles and dispersed in the solvent. By contrast, the pre-mixed powder oxidized at temperatures above 300 °C sinks promptly in the solvent. It is evident that the physically deposited Co_3O_4 particles are detached from the Ni particles when the pre-mixed powder is added to the slurry, and this causes agglomeration of cobalt during the mixing and annealing process. Therefore, an additional heat-treatment step is required before mixing to diminish the separation of n-Co_3O_4 from Ni.

To elucidate the structure of the pre-mixed powder, XRD experiments were performed. The XRD patterns of the pristine NiO and n-Co_3O_4-deposited Ni powder prior to and after annealing at 650 °C are presented in Fig. 4. The XRD pattern of the pristine NiO, which was prepared by the oxidation of the Ni powder at 650 °C as a reference, is given in Fig. 4(a), and the diffraction pattern is assigned to a rock-salt crystalline structure. The pre-mixed powder before oxidation shows a combination of metallic Ni (*Fm3m* structure) and cubic spinel Co_3O_4 diffraction features, as shown in Fig. 4(b). After oxidation, however, the metallic Ni features completely disappear and NiO features appear, as indicated in Fig. 4(c). It is noteworthy that the diffraction features of Co_3O_4 completely vanish after oxidation and this provides strong evidence that the pre-mixed powder forms a (Co, Ni)O solid solution after the oxidation process at 650 °C. It has been reported that a Ni and Co oxide binary system, whose cobalt content is less than 15 mol%, forms a solid solution at 650 °C in air [28], which is in good agreement with the present results. Rietveld refinements were performed for the XRD patterns of the pristine and Co-containing NiO. The lattice parameters of the pristine and Co-containing NiO are 4.174 and 4.180 Å, respectively. The increase in the lattice parameter of the Co-containing NiO is attributed to the size of Co^{2+} (0.75 Å), which is larger than that of Ni^{2+} (0.69 Å) [29]. Therefore, this heat-treatment plays an important role in converting the physically bound mixed oxide system to a chemically bound solid solution system and preventing the separation of n-Co_3O_4 from Ni.

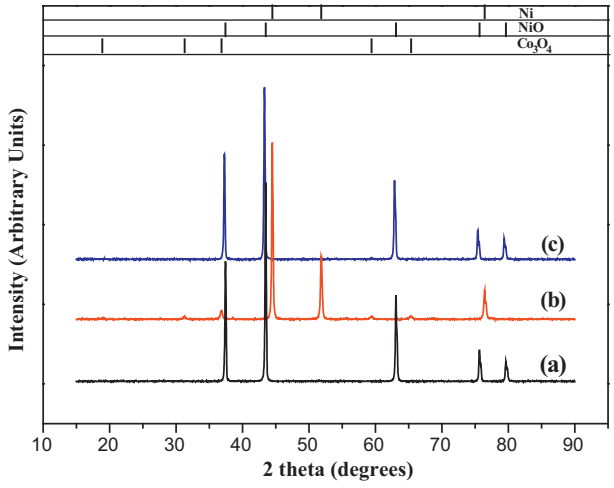

Fig. 4. XRD pattern collected from (a) n-Co_3O_4 (10 mol%) deposited Ni powder (before oxidation), (b) $Ni_{0.9}Co_{0.1}O$ powder (after oxidation of (a) at 650 °C), (c) pristine NiO (Ni after oxidation at 650 °C). Bragg peak position obtained from JCPDS cards (Ni: 04-0850, NiO: 47-1049, and Co_3O_4: 42-1467).

3.3. Characteristics of modified materials, $Ni_{0.9}Co_{0.1}O$

In order to examine the properties of the modified material, $Ni_{0.9}Co_{0.1}O$ was further investigated by means of various techniques. Electrochemical impedance spectroscopy was performed to characterize the electrochemical properties of the modified material. The electrochemical impedance spectra of the pristine NiO and $Ni_{0.9}Co_{0.1}O$ in $(Li_{0.62}K_{0.38})_2CO_3$ at 650 °C under a CO_2/O_2 (0.67/0.33 atm) atmosphere are shown in Fig. 5. Both spectra have two semi-arcs that are overlapping. The arc observed in the high-

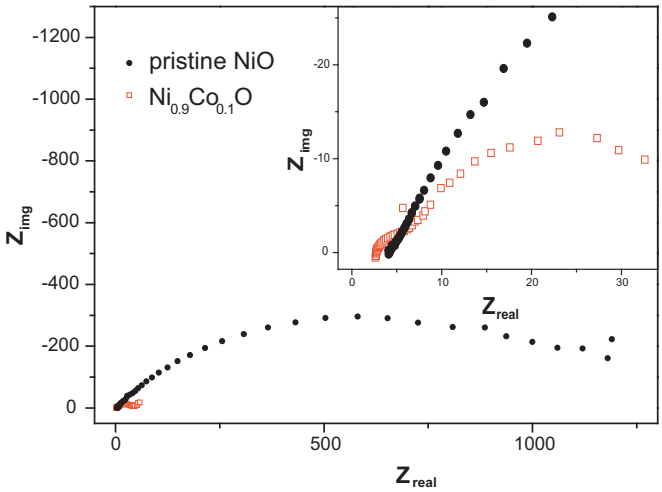

Fig. 5. EIS spectra of NiO and $Ni_{0.9}Co_{0.1}O$ after immersion in $(Li_{0.62}K_{0.38})_2CO_3$ at 650 °C for 100 h.

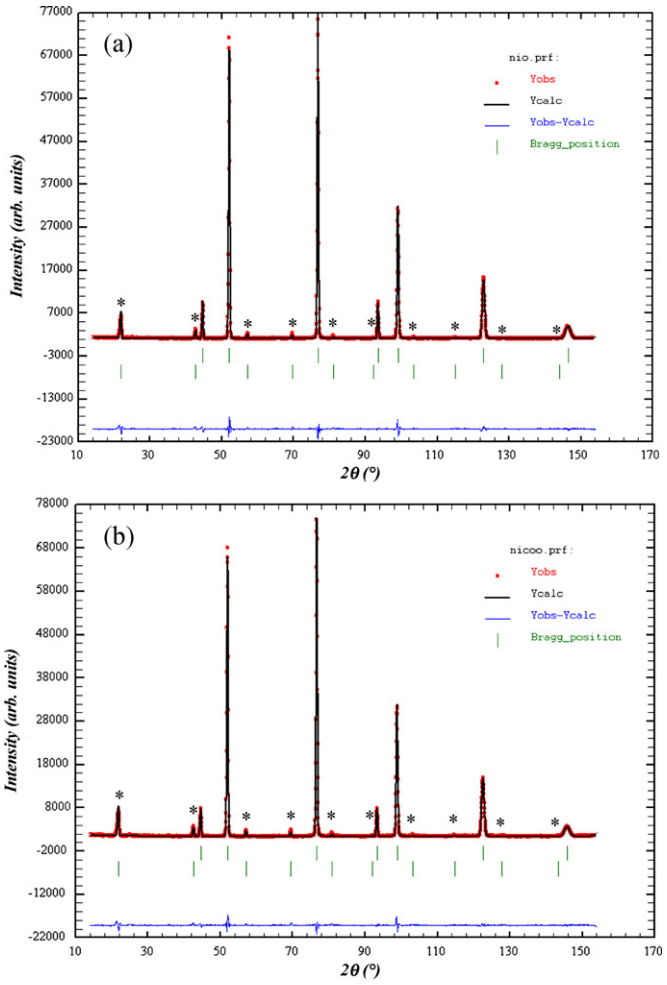

Fig. 6. Neutron diffraction pattern collected from (a) NiO and (b) $Ni_{0.9}Co_{0.1}O$.

frequency region is associated with the bulk resistance (R_{bulk}), which is related to the electrode materials and the gold lead, and the arc in the low-frequency region is attributed to the charge-transfer resistance (R_{CT}) for the oxygen reduction reaction. The data in Fig. 5 unambiguously demonstrate that $Ni_{0.9}Co_{0.1}O$ has a significantly lower charge-transfer resistance, due to the higher degree of lithiation of $Ni_{0.9}Co_{0.1}O$. Escudero et al. [30] reported that lithiation of NiO reduces the charge-transfer resistance by one or two order(s) of magnitude in comparison with the pristine NiO. Both materials exhibit significantly decreased charge-transfer resistances compared with unlithiated samples. The charge-transfer resistance of NiO, however, is still much higher than that of $Ni_{0.9}Co_{0.1}O$.

Neutron diffraction was employed to investigate the structural changes of the modified cathode materials. This technique has several advantages over XRD. The most important one is that scattering cross-section of neutron diffraction has no relevance to the atomic number. Because the materials investigated in this study are composed of Li, Co and Ni, and Li has a quite small scattering cross-section, it is difficult to determine the accurate contents of the Li-containing phases using XRD. Moreover, it is difficult to separate the individual contributions of Ni and Co in the XRD pattern accurately because the scattering factor of Co is similar to that of Ni. By contrast, the neutron scattering factors for Li, Co and Ni are quite different and, therefore, neutron diffraction is a suitable tool to investigate this system. As shown in Fig. 6 and Table 1, the diffraction patterns of the $Ni_{0.9}Co_{0.1}O$ and pristine NiO are assigned to rock-salt structures. Additional diffraction features, which were not

Table 1
Rietveld refinement results obtained from neutron diffraction patterns of NiO and $Ni_{0.9}Co_{0.1}O$.

	Lattice parameter (Å)	Occupancy		
		Ni	Co	O[a]
NiO	4.1776	1	–	1
$Ni_{0.9}Co_{0.1}O$	4.1844	0.899	0.101	1

[a] Occupancy of oxygen is fixed at 1.

detected in XRD, are observed, and these peaks are attributed to the magnetic reflection of NiO (denoted by asterisk), as shown in Fig. 6. Corresponding to the XRD result, the neutron diffraction patterns of $Ni_{0.9}Co_{0.1}O$ do not show any features related to the Co_3O_4 phase, and the lattice parameter is determined to be 4.1844 Å, which is slightly larger than that of NiO (4.1776 Å). According to Vegard's law, the lattice parameter of a solid solution varies linearly within those of the constituents as a function of its composition. The lattice parameters of NiO and CoO are 4.177 and 4.261 Å, respectively (from JCPDS cards 47-1049 and 48-1719), and the theoretical value of $Ni_{0.9}Co_{0.1}O$, calculated from the reference values, is 4.1854 Å, which is good agreement with our result (4.1844 Å). Therefore, it can be concluded that the Co and Ni oxides form a solid solution after oxidation at 650 °C.

Lithiated $Ni_{0.9}Co_{0.1}O$ and NiO were also investigated by neutron diffraction. The neutron diffraction patterns of $Ni_{0.9}Co_{0.1}O$ and NiO immersed in $(Li_{0.68}K_{0.32})_2CO_3$ at 650 °C in a CO_2:O_2 (0.67:0.33 atm) atmosphere for 100 h are given in Fig. 7. The neutron diffraction peaks after lithiation are slightly shifted toward a higher angle in comparison with the unlithiated samples. As lithium is doped into it, NiO turns into $Li_xNi^{2+}_{1-2x}Ni^{3+}_xO$, and the lattice parameter is reduced since the sum of the ionic radii of two Ni^{2+} (0.69 Å) ions is larger than that of the Li^+ (0.76 Å) and Ni^{3+}(0.56 Å) ions [28]. The lattice parameter of the lithiated NiO immersed for 100 h is determined to be 4.1759 Å, which is smaller than that of un-lithiated NiO (4.1776 Å), and the occupancy of Li is about 2.0%. The refined profile of the lithiated $Ni_{0.9}Co_{0.1}O$ is not, however, in accordance with the experimental data obtained by neutron diffraction, as shown in Fig. 7(b). The detailed neutron diffraction pattern of the lithiated $Ni_{0.9}Co_{0.1}O$ is shown in detail in Fig. 7(c), and asymmetric features are clearly observed. The right side of each peak is much broader than the left side, and it is obvious that the broadness of the peaks becomes more significant as the scattering angle increases. It is unambiguously suggested that an additional phase, which has a slightly smaller lattice parameter, is present. The Rietveld refinement results for the lithiated $Ni_{0.9}Co_{0.1}O$, given in Fig. 7(d) and Table 2, indicate that it consists of two phases. One of these phases has a cubic lattice parameter of 4.1817 Å and a Li concentration of 1.6%, whereas the corresponding values of the other phase are 4.1616 Å and 6.7%, respectively. It is quite interesting that the concentration of Li is 6.7%, because the Li concentration in a NiO cathode, which is in situ oxidized and lithiated at 650 °C, is generally about 2–4 mol% [15]. In addition, the lattice parameter decreases with increasing concentration of Li, due to the smaller ionic radius of Li ions compared with that of Ni ions [29]. From the quantitative analysis, the fractions of each phase are determined to be 34.6 and 65.4% for the high (6.7%) and low (1.6%) concentrations of Li, respectively. The total Li concentration of the lithiated $Ni_{0.9}Co_{0.1}O$ is 3.4%, taking into consideration all of the phases. Surprisingly, this value is significantly higher than that of the lithiated NiO (2.0%) and corresponds to that of lithiated NiO after MCFC operation for 2000 h, as shown in Table 2.

The SEM images of NiO and $Ni_{0.9}Co_{0.1}O$ after lithiation for 100 h are presented in Fig. 8. The morphology of unlithiated NiO and $Ni_{0.9}Co_{0.1}O$ is smooth and round, whereas lithiated NiO and $Ni_{0.9}Co_{0.1}O$ consist of horn-like, edged particles. Fukui et al. [15]

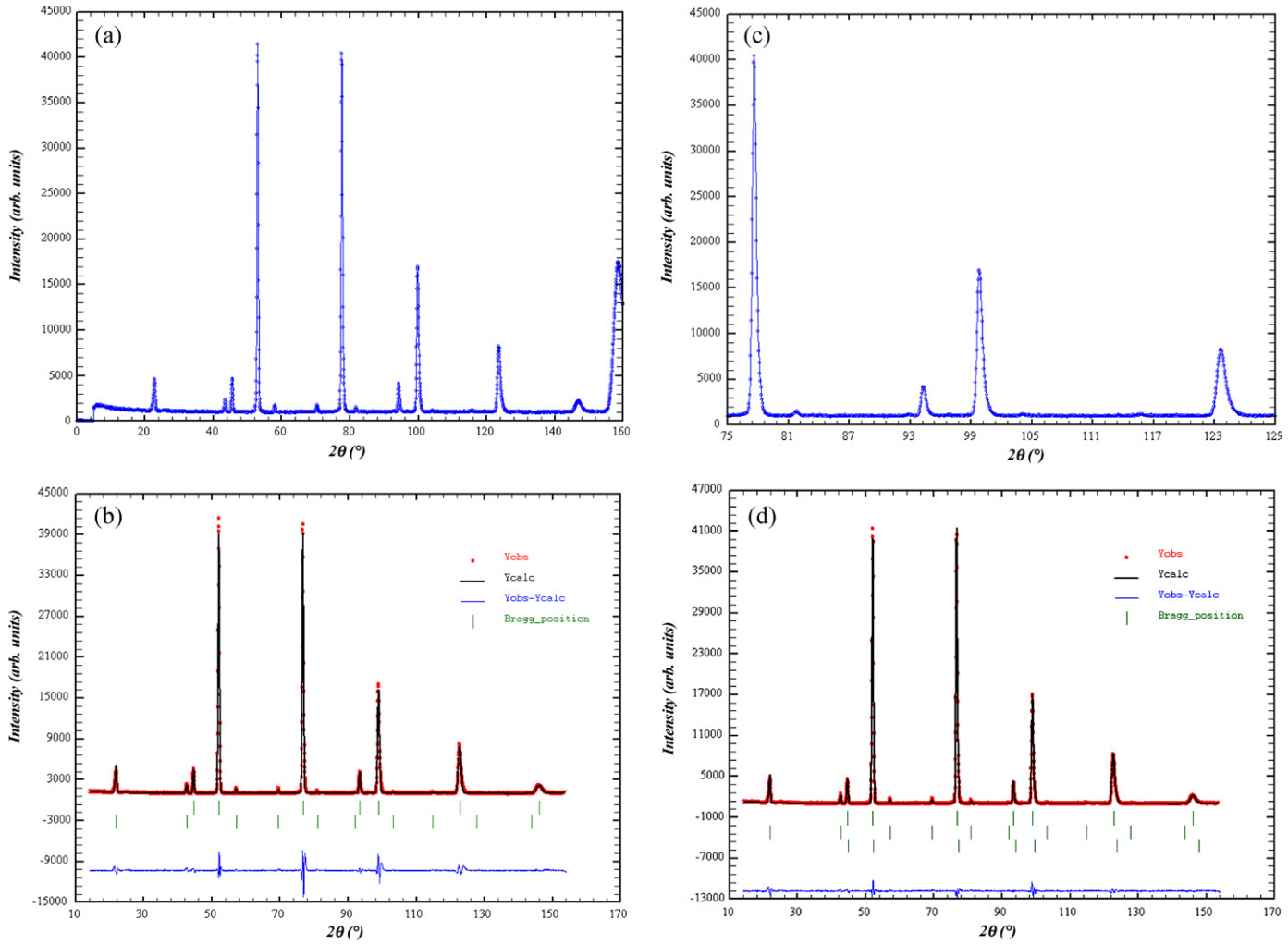

Fig. 7. Neutron diffraction pattern and refinement profile of lithiated $Ni_{0.9}Co_{0.1}O$ in $(Li_{0.62}K_{0.38})_2CO_3$ at 650 °C under CO_2/O_2 = 0.67/0.33 atm after 100 h; (a) neutron diffraction pattern, (b) enlarged view of (a), (c) refinement profile using 1 phase, and (d) refinement profile using two phases.

reported the formation of hexagonal crystals on the surface of the grains for lithiated CoO/NiO composites. Lithiated $Ni_{0.9}Co_{0.1}O$ has a sharper-edged shape than lithiated NiO, as shown in Fig. 8(a) and (b), respectively, since the concentration of Li in lithiated $Ni_{0.9}Co_{0.1}O$ is higher than that in lithiated NiO after 100 h. SEM images of the cross-section of the $Ni_{0.9}Co_{0.1}O$ cathode after lithiation for 300 h are given in Fig. 8(c) and (d). A core–shell structure is clearly observed. The inner phase is spherical, while the outer phase has an edge shape. As explained above, neutron diffraction data demonstrate the presence of two different phases in the lithiated $Ni_{0.9}Co_{0.1}O$. These two different phases, which are clearly observed in the SEM images, are consistent with the neutron diffraction analysis. The outer phase, having an edge shape, corresponds to the more lithiated phase observed by neutron diffraction analysis, while the inner phase is the less lithiated phase with a spherical shape. In fact, the presence of a highly lithiated phase will affect the electrochemical activity and stability because the dissolution of the cathode material and the electrochemical reactions occur at the surface. The surface region retains a high concentration of Li in comparison with the bulk region, and therefore, it can act as a barrier for the bulk phase because the highly lithiated phase is more stable in molten carbonates.

Solubility tests were performed in $(Li_{0.62}K_{0.38})_2CO_3$ at 650 °C under CO_2/O_2 (0.67/0.33 atm) for 300 h in order to confirm the stability of the $Ni_{0.9}Co_{0.1}O$ cathode. The concentration of Ni in the carbonates was determined by ICP-MS. The Ni solubility of the

Table 2
Rietveld refinement results obtained from neutron diffraction patterns of lithiated NiO and lithiated $Ni_{0.9}Co_{0.1}O$ after immersion for 100 h and lithiated NiO after cell operation for 2000 h.

	Lattice parameter (Å)	Occupancy			
		Ni	Co	Li	O[b]
In situ lithiation NiO (100 h)	4.1759	0.980	–	0.020	1
In situ lithiation $Ni_{0.9}Co_{0.1}O$ (100 h)	4.1817 (65.4%)[a]	0.885	0.098	0.016	1
	4.1616 (34.6%)[a]	0.839	0.093	0.067	1
In situ lithiation NiO (2000 h)	4.1731	0.966	–	0.034	1

[a] Percentage indicates fraction of each phase in lithiated $Ni_{0.9}Co_{0.1}O$.
[b] Occupancy of oxygen is fixed at 1.

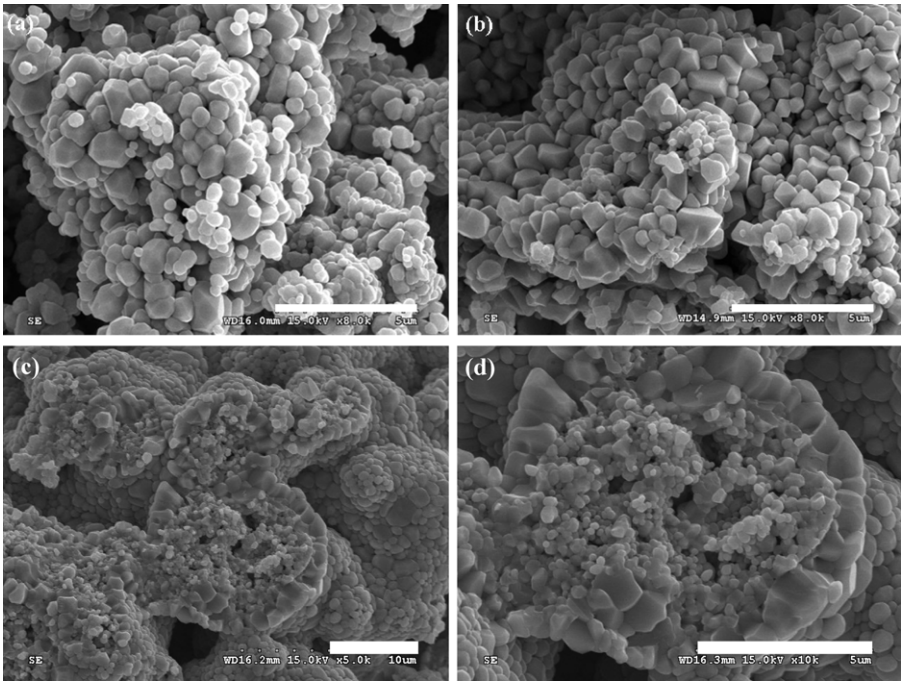

Fig. 8. SEM images of (a) NiO and (b) $Ni_{0.9}Co_{0.1}O$ after lithiation under cathodic conditions for 100 h. SEM images of cross-section of $Ni_{0.9}Co_{0.1}O$ cathode after lithiation for 300 h; (c) SEM image and (d) enlarged view of (c).

$Ni_{0.9}Co_{0.1}O$ and pristine NiO cathodes in the molten carbonate mixture is shown in Fig. 9. The Ni solubility of the pristine NiO cathode is 30.35 ppm, while that of the modified sample is 8.311 ppm, which is lower than that of the Co-coated NiO cathode (12.71 ppm) [23]. It has been reported that the higher Li concentration of the lithiated cathode improves its stability [30,31]. Since a high concentration of Li indicates a high content of Ni^{3+}, the chemical binding of Ni and O can be strengthened. Specifically, the interaction between Ni^{3+} and O^{2-} would be stronger than that between Ni^{2+} and O^{2-}. As a result, highly lithiated NiO could reduce the solubility of Ni and enhance the stability of the electrode in the molten carbonates. In summary, the presence of cobalt in the lithiation process results in the formation of a highly lithiated phase on the surface that is quite stable in the molten carbonate mixture, since a trivalent metal can bind more strongly with oxygen. Consequently, the phase reduces the dissolution of the cathode and thereby acts as a barrier.

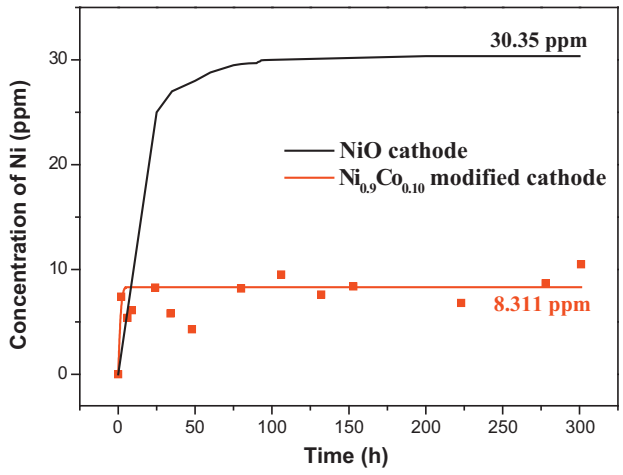

Fig. 9. Solubility of pristine NiO and $Ni_{0.9}Co_{0.1}O$ cathode in $(Li_{0.62}K_{0.38})_2CO_3$ at 650 °C under CO_2/O_2 = 0.67/0.33 atm for 300 h.

4. Conclusion

A modified NiO powder has been prepared from Co_3O_4 nanoparticles, without any complex process, for use as the cathode material for MCFCs. The direct addition of pre-mixed *n*-Co_3O_4 and Ni powders to a slurry results in the agglomeration of cobalt. To prevent this agglomeration, a pre-mixed powder is annealed before it is mixed with the slurry. It is observed that *n*-Co_3O_4 is not separated from Ni when the pre-mixed powder is annealed at temperatures above 300 °C. In addition, cobalt is evenly distributed without agglomeration. The morphology of the modified powder is similar to that of the Co-coated powder, and it forms a $Ni_{0.9}Co_{0.1}O$ solid solution at 650 °C. From the lithiation test, it is found that $Ni_{0.9}Co_{0.1}O$ is more lithiated than the pristine NiO cathode, and the Ni solubility of the modified cathode is ~8.311 ppm after 300 h. Moreover, it is found that lithiated $Ni_{0.9}Co_{0.1}O$ has two different structures, which have different contents of Li. The highly lithiated phase completely covers the particles, and the modified cathode is more stable than the pristine NiO cathode under the operating conditions of an MCFC. This enhancement in stability is attributed to the high degree of lithiation afforded by the addition of cobalt because the formation of trivalent metal ions in the material causes them to strongly bind with the oxygen ions. Ultimately, the phase reduces dissolution of the cathode material by acting as a barrier. The newly prepared cathode material demonstrates good electrochemical properties and chemical stability in the electrolyte, and the technique can be applied to mass-production.

Acknowledgements

The authors are gratefully for the support of the Korea Electric Power Corporation in this work. C.W.Y. also acknowledges a Sungshin Women's University Research Grant in 2010.

References

[1] S.T. Kuk, Y.S. Song, K. Kim, J. Power Sources 83 (1999) 50–56.
[2] Q.M. Nguyen, J. Power Sources 24 (1988) 1–19.

[3] S.-G. Kim, S.P. Yoon, J. Han, S.W. Nam, T.H. Lim, I.-H. Oh, S.-A. Hong, Electrochim. Acta 49 (2004) 3081–3089.
[4] A. Lundblad, S. Schwartz, B. Bergman, J. Power Sources 90 (2000) 224–230.
[5] C. Milanese, V. Berbenni, G. Bruni, A. Marini, G. Chiodelli, M. Villa, Solid State Ionics 177 (2006) 1893–1896.
[6] A. Ringuedé, A. Wijayasinghe, V. Albin, C. Lagergren, M. Cassir, B. Bergman, J. Power Sources 160 (2006) 789–795.
[7] T.M.T.N. Tennakoon, G. Lindbergh, B. Bergman, J. Electrochem. Soc. 144 (1997) 2296–2301.
[8] A. Wijayasinghe, B. Bergman, C. Lagergren, Electrochim. Acta 49 (2004) 4709–4717.
[9] A. Wijayasinghe, B. Bergman, C. Lagergren, Solid State Ionics 177 (2006) 175–184.
[10] A. Wijayasinghe, B. Bergman, C. Lagergren, Solid State Ionics 177 (2006) 165–173.
[11] A. Wijayasinghe, C. Lagergren, B. Bergman, Fuel Cells 2 (2002) 181–188.
[12] M.J. Escudero, X.R. Nóvoa, T. Rodrigo, L. Daza, J. Power Sources 106 (2002) 196–205.
[13] M.J. Escudero, T. Rodrigo, L. Daza, Catal. Today 107–108 (2005) 377–387.
[14] M.J. Escudero, T. Rodrigo, J. Soler, L. Daza, J. Power Sources 118 (2003) 23–34.
[15] T. Fukui, S. Ohara, H. Okawa, T. Hotta, M. Naito, J. Power Sources 86 (2000) 340–346.
[16] T. Fukui, H. Okawa, T. Tsunooka, J. Power Sources 71 (1998) 239–243.
[17] P. Ganesan, H. Colon, B. Haran, R. White, B.N. Popov, J. Power Sources 111 (2002) 109–120.
[18] M.Z. Hong, S.C. Bae, H.S. Lee, H.C. Lee, Y.-M. Kim, K. Kim, Electrochim. Acta 48 (2003) 4213–4221.
[19] B. Huang, Q.-C. Yu, H.-M. Wang, G. Chen, K.-A. Hu, J. Power Sources 137 (2004) 163–174.
[20] M.H. Kim, M.Z. Hong, Y.-S. Kim, E. Park, H. Lee, H.-W. Ha, K. Kim, Electrochim. Acta 51 (2006) 6145–6151.
[21] S.-G. Kim, S.P. Yoon, J. Han, S.W. Nam, T.-H. Lim, S.-A. Hong, H.C. Lim, J. Power Sources 112 (2002) 109–115.
[22] S.T. Kuk, Y.S. Song, S. Suh, J.Y. Kim, K. Kim, J. Mater. Chem. 11 (2001) 630–635.
[23] H. Lee, M. Hong, S. Bae, H. Lee, E. Park, K. Kim, J. Mater. Chem. 13 (2003) 2626–2632.
[24] H.S. Lee, M.Z. Hong, E.J. Park, K. Kim, J. Mater. Sci. 39 (2004) 5595–5598.
[25] H. Okawa, J.H. Lee, T. Hotta, S. Ohara, S. Takahashi, T. Shibahashi, Y. Yamamasu, J. Power Sources 131 (2004) 251–255.
[26] E. Park, M. Hong, H. Lee, M. Kim, K. Kim, J. Power Sources 143 (2005) 84–92.
[27] L. Giorgi, M. Carewska, M. Patriarca, S. Scaccia, E. Simonetti, A. Di Bartolomeo, J. Power Sources 49 (1994) 227–243.
[28] R.J. Moore, J. White, J. Mater. Sci. 9 (1974) 1393–1400.
[29] R.D. Shannon, Acta Crystallogr. A 32 (1976) 751–767.
[30] M.J. Escudero, X.R. Nóvoa, T. Rodrigo, L. Daza, J. Appl. Electrochem. 32 (2002) 929–936.
[31] K. Takizawa, A. Hagiwara, J. Electrochem. Soc. 148 (2001) A1034–A1040.